J|A|C|S ARTICLES

Published on Web 11/03/2009

Near-IR Femtosecond Transient Absorption Spectroscopy of Ultrafast Polaron and Triplet Exciton Formation in Polythiophene Films with Different Regioregularities

Jiamo Guo, Hideo Ohkita,* Hiroaki Benten, and Shinzaburo Ito

Department of Polymer Chemistry, Graduate School of Engineering, Kyoto University, Katsura, Nishikyo, Kyoto 615-8510, Japan

Received August 5, 2009; E-mail: ohkita@photo.polym.kyoto-u.ac.jp

Abstract: The formation dynamics of polaron pairs, polarons, and triplet excitons in regiorandom and regioregular poly(3-hexylthiophene) (RRa-P3HT and RR-P3HT) films was comprehensively studied by transient absorption spectroscopy over the wide wavelength region from 500 to 1650 nm under various excitation intensities. In both RRa-P3HT and RR-P3HT films, polaron pairs were generated not from relaxed singlet exciton states but from hot excitons on a time scale of <100 fs and decayed monomolecularly by geminate recombination. In RRa-P3HT films, triplet excitons were rapidly generated on a picosecond time scale from higher exciton states produced by the singlet exciton−exciton annihilation as well as from the lowest singlet exciton states by the normal intersystem crossing. In RR-P3HT films, no triplet excitons were observed; polarons were also generated not from relaxed singlet exciton states but from hot excitons in competition with the formation of polaron pairs. The polarons formed in RR-P3HT can freely migrate and mainly recombine with other polarons bimolecularly in the nanosecond time domain. The ultrafast formation of triplet excitons can be explained by the singlet exciton fission into two triplets, and the ultrafast formation of polaron pairs and polarons can be explained on the basis of the hot-exciton dissociation model where the excess thermal energy of the initially formed hot excitons is necessary to overcome their Coulombic binding energy. The remarkably different formation dynamics in P3HTs with different regioregularities is discussed in terms of the film morphology of conjugated polymers.

1. Introduction

Conjugated polymers are attracting extensive academic and commercial interest because of the potential optoelectronic applications such as field-effect transistors (FETs),[1,2] solar cells,[3−5] and light-emitting diodes.[6] Of the many conjugated polymers, poly(3-hexylthiophene) (P3HT) has attracted considerable attention due to its good solubility, processability, stability, and unique optoelectronic properties. For P3HT, the 3-hexyl substituent in a thiophene ring can be incorporated into a polymer chain with two different regioregularities: head-to-tail (HT) and head-to-head (HH). Of particular interest is the regularly substituted poly(3-hexylthiophene) (RR-P3HT), in which the hexyl side chain is attached to the third position of a thiophene ring in an HT regioregularity, because self-organization of RR-P3HT chains results in two-dimensional (2D) lamella nanostructures that are different from the traditional one-dimensional (1D) polymer chains. In such a self-organized 2D lamella structure, the interchain distance is as short as ∼3.8 Å, resulting in strong interchain interaction.[7,8] In contrast, irregularly substituted P3HT (RRa-P3HT) forms disordered amorphous films with a glass transition temperature of $T_g \approx -3$ °C,[9] because unfavorable HH couplings cause a sterically driven twist of the thiophene rings, resulting in shorter conjugation. In other words, the regioregularity has a critical impact on the self-organization and nanostructures of polymer chains and therefore on macroscopic device performances such as FETs[7] and solar cells[10,11] based on P3HTs.

Recent spectroscopic studies on P3HTs have shown that photoexcitations such as excitons and polarons are strongly dependent upon the regioregularity. Because of the strong interchain interaction in RR-P3HT films, singlet excitons are more delocalized to form interchain excitons, whereas intrachain singlet excitons are formed in RRa-P3HT films and substantially

(1) Braga, D.; Horowitz, G. *Adv. Mater.* **2009**, *21*, 1473–1486.
(2) Chabinyc, M. L.; Jimison, L. H.; Rivnay, J.; Salleo, A. *MRS Bull.* **2008**, *33*, 683–689.
(3) Günes, S.; Neugebauer, H.; Sariciftci, N. S. *Chem. Rev.* **2007**, *107*, 1324–1338.
(4) Brabec, C. J.; Durrant, J. R. *MRS Bull.* **2008**, *33*, 670–675.
(5) Thompson, B. C.; Fréchet, J. M. J. *Angew. Chem., Int. Ed.* **2008**, *47*, 58–77.
(6) So, F.; Kido, J.; Burrows, P. *MRS Bull.* **2008**, *33*, 663–669.
(7) Sirringhaus, H.; Brown, P. J.; Friend, R. H.; Nielsen, M. M.; Bechgaard, K.; Langeveld-Voss, B. M. W.; Spiering, A. J. H.; Janssen, R. A. J.; Meijer, E. W.; Herwig, P.; de Leeuw, D. M. *Nature* **1999**, *401*, 685–688.
(8) Chen, T.-A.; Wu, X.; Rieke, R. D. *J. Am. Chem. Soc.* **1995**, *117*, 233–244.
(9) Hugger, S.; Thomann, R.; Heinzel, T.; Thurn-Albrecht, T. *Colloid Polym. Sci.* **2004**, *282*, 932–938.
(10) Kim, Y.; Cook, S.; Tuladhar, S. M.; Choulis, S. A.; Nelson, J.; Durrant, J. R.; Bradley, D. D. C.; Giles, M.; Mcculloch, I.; Ha, C.-S.; Ree, M. *Nat. Mater.* **2006**, *5*, 197–203.
(11) Woo, C. H.; Thompson, B. C.; Kim, B. J.; Toney, M. F.; Fréchet, J. M. J. *J. Am. Chem. Soc.* **2008**, *130*, 16324–16329.

10.1021/ja906621a CCC: $40.75 © 2009 American Chemical Society

converted to triplet excitons.[12,13] The long-lived polarons are also delocalized among adjacent chains, forming interchain polarons as well as intrachain polarons in RR-P3HT films, whereas only intrachain polarons are formed in RRa-P3HT films.[13,14] Charge modulation spectroscopy of P3HT-based FETs has shown a higher fraction of interchain polarons in the FET device using RR-P3HT with higher regioregularity.[7] These studies demonstrated that higher hole mobilities observed for RR-P3HT-based FETs are due to 2D charge transport enhanced by interchain polarons in the self-organized lamellae. In other words, spectroscopic studies are useful for understanding the relationship between macroscopic properties such as hole mobility and microscopic transient species such as polarons.

Although previous spectroscopic studies have provided information on such transient species generated in RR-P3HT and RRa-P3HT films, the formation dynamics of these transient species is not fully understood. In particular, the formation dynamics of polarons from excitons should play a central role in P3HT-based solar cells whose active layer is considered to consist of partially crystalline and amorphous domains of P3HT and nanocrystals of a fullerene derivative (PCBM).[15,16] Recently, several groups have reported that polarons may be generated not only at the heterojunction but also in the P3HT bulk.[17−20] Therefore, this study will provide an in-depth understanding of the mechanism of charged carrier generation in P3HT-based solar cells. Herein we report a comprehensive spectroscopic study on the formation dynamics of various photoexcitations in P3HT with different regioregularities: RR-P3HT films are employed as a model of the self-organized 2D lamella structure, and RRa-P3HT films are employed as a model of the amorphous structure. To distinguish each transient species and trace them immediately after the laser excitation, we measured femtosecond transient absorption over the wide wavelength region from 500 to 1650 nm. Although there are characteristic absorption bands of the primary photoexcitations in the near-IR wavelength, most of the femtosecond transient absorption studies have been conducted in a limited wavelength range up to ∼1100 nm. The primary motivation of this study is a fundamental understanding of the photophysics of polythiophene films with different regioregularities, but the relevance of the photophysics to polymer solar cells is also mentioned.

2. Results

2.1. RRa-P3HT. 2.1.1. Transient Absorption Spectra. Figure 1 shows transient absorption spectra of RRa-P3HT films measured from −100 fs to +3 ns. Upon the excitation at 400 nm, as shown in Figure 1a, a small absorption peak and a broad absorption band were observed at around 700 and 900 nm, respectively, at −100 fs. On the picosecond time scale, the small absorption band decayed with time while the broad absorption band increased and then decayed with the peak red-shifted from 900 to 1060 nm. At a later time stage, both absorption bands disappeared, and instead a new absorption band was observed at around 800 nm and decayed slowly. Upon the excitation at 500 nm, as shown in Figure 1c, only a broad band was observed at around 1000 nm but no absorption was observed at around 700 nm at −100 fs. Similarly to the 400 nm excitation, the broad absorption band decayed with the peak red-shifted from 1000 to 1060 nm on the picosecond time scale, and then a new absorption band was observed at around 800 nm and decayed slowly at a later time stage.

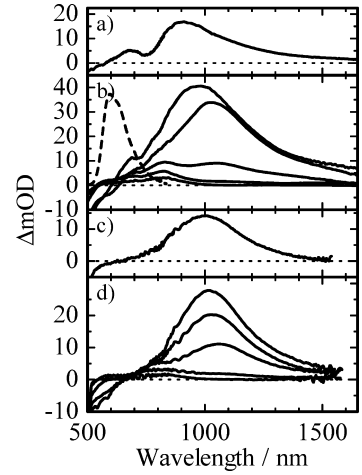

Figure 1. Femtosecond transient absorption spectra of RRa-P3HT films excited at 400 nm (∼30 μJ cm^{-2}) measured at (a) −100 fs and (b) 0, 1, 10, 100, and 3000 ps from top to bottom and excited at 500 nm (∼20 μJ cm^{-2}) measured at (c) −100 fs and (d) 0, 1, 10, 100, and 3000 ps from top to bottom. The broken line represents the fluorescence spectrum of the RRa-P3HT film.

The broad absorption band at around 1000 nm showed the same decay dynamics as the negative signal at 600 nm at an early time stage. The negative signal is attributable to stimulated emission of RRa-P3HT because the wavelength corresponded to the fluorescence band of the RRa-P3HT film as shown by the broken line in Figure 1b. Therefore, the absorption band at around 1000 nm is assigned to singlet excitons of RRa-P3HT. This assignment is consistent with previous reports[12,13] although the peak wavelength was slightly different as will be discussed later.

As shown in Figure 2, the long-lived absorption band at around 800 nm was still observed even on the microsecond time scale, and decayed monoexponentially with a lifetime of 7 μs under an Ar atmosphere at room temperature but much faster under an O_2 atmosphere as shown in the inset of this figure. Thus, the absorption band at around 800 nm is ascribed to triplet excitons of RRa-P3HT. No other long-lived transients were observed under an excitation intensity of 30 μJ cm^{-2}.

On the other hand, the absorption band at around 700 nm was so small that it was difficult to distinguish it from the other two bands. Figure 3 shows transient absorption spectra at 100 ps monitored with a probe light polarized in the direction parallel (solid line) or perpendicular (broken line) to the polarization direction of the excitation light at 400 nm. From the polarized

(12) Korovyanko, O. J.; Österbacka, R.; Jiang, X. M.; Vardeny, Z. V.; Janssen, R. A. J. *Phys. Rev. B* **2001**, *64*, 235122.
(13) Jiang, X.; Österbacka, R.; Korovyanko, O.; An, C. P.; Horovitz, B.; Janssen, R. A. J.; Vardeny, Z. V. *Adv. Funct. Mater.* **2002**, *12*, 587–597.
(14) Österbacka, R.; An, C. P.; Jiang, X. M.; Vardeny, Z. V. *Science* **2000**, *287*, 839–842.
(15) Erb, T.; Zhokhavets, U.; Gobsch, G.; Raleva, S.; Stühn, B.; Schilinsky, P.; Waldauf, C.; Brabec, C. J. *Adv. Funct. Mater.* **2005**, *15*, 1193–1196.
(16) Yang, X.; Loos, J.; Veenstra, S. C.; Verhees, W. J. H.; Wienk, M. M.; Kroon, J. M.; Michels, M. A. J.; Janssen, R. A. J. *Nano Lett.* **2005**, *5*, 579–583.
(17) Sheng, C.-X.; Tong, M.; Singh, S.; Vardeny, Z. V. *Phys. Rev. B* **2007**, *75*, 085206.
(18) Piris, J.; Kopidakis, N.; Olson, D. C.; Shaheen, S. E.; Ginley, D. S.; Rumbles, G. *Adv. Funct. Mater.* **2007**, *17*, 3849–3857.
(19) Cook, S.; Furube, A.; Katoh, R. *Energy Environ. Sci.* **2008**, *1*, 294–299.
(20) Piris, J.; Dykstra, T. E.; Bakulin, A. A.; van Loosdrecht, P. H. M.; Knulst, W.; Trinh, M. T.; Schins, J. M.; Siebbeles, L. D. A. *J. Phys. Chem. C* **2009**, *113*, 14500–14506.

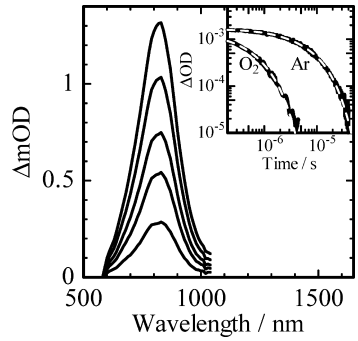

Figure 2. Microsecond transient absorption spectra of RRa-P3HT films measured at 0.5, 2, 4, 6, and 10 μs from top to bottom. The inset shows transient absorption decays at 850 nm under Ar and O_2 atmospheres. The broken lines represent fitting curves with a monoexponential equation: $\Delta OD \propto \exp(-t/\tau)$. The excitation wavelength was 450 nm ($\sim$30 μJ cm^{-2}).

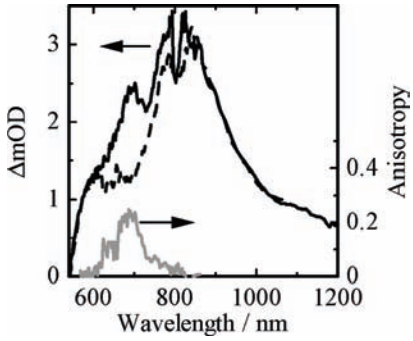

Figure 3. Femtosecond transient absorption spectra of RRa-P3HT films monitored with a probe light polarized in the direction parallel (solid line, $\Delta OD_{||}$) or perpendicular (broken line, $\Delta OD_{\perp}$) to the polarization direction of the excitation light at 100 ps. The anisotropy spectrum (gray line) is calculated by $r(t) = (\Delta OD_{||} + \Delta OD_{\perp})/(\Delta OD_{||} - 2\Delta OD_{\perp})$. The excitation wavelength was 400 nm ($\sim$30 μJ cm^{-2}).

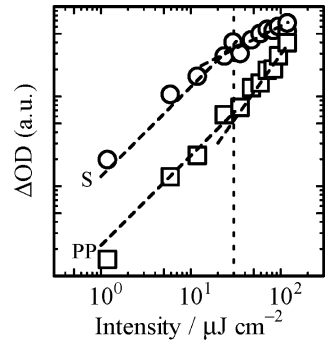

Figure 4. Log−log plots of the initial transient signals of RRa-P3HT films at 1000 nm (singlet exciton, S; open circles) and 650 nm (polaron pair, PP; open squares) against the excitation intensity. The broken lines represent fitting curves with a power-law equation: $\Delta OD \propto I^{\alpha}$. The dotted line exhibits the turning point from linear to nonlinear dependence of the transient signals ($\sim$30 μJ cm^{-2}).

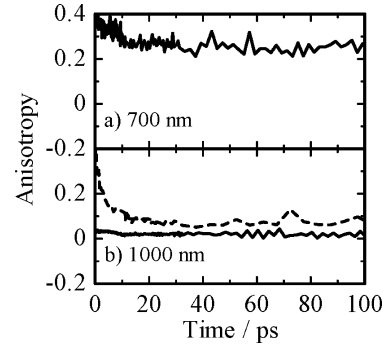

Figure 5. Femtosecond transient anisotropy decays of RRa-P3HT films monitored at (a) 700 nm and (b) 1000 nm. The anisotropy is calculated by $r(t) = (\Delta OD_{||} + \Delta OD_{\perp})/(\Delta OD_{||} - 2\Delta OD_{\perp})$. The excitation wavelengths were 400 nm (solid lines, $\sim$30 μJ cm^{-2}) and 500 nm (broken line, $\sim$20 μJ cm^{-2}).

transient absorption spectra, the anisotropy spectrum (solid gray line) was calculated by the following equation: $r(t) = (\Delta OD_{||} + \Delta OD_{\perp})/(\Delta OD_{||} - 2\Delta OD_{\perp})$. As shown in this figure, both spectra were almost the same at around 800 nm but distinctly different at around 700 nm: $r \approx 0.25$ at 700 nm and $r \approx 0$ at 800 nm. This result suggests that the 700 nm band should be assigned to a species different from triplet excitons. Rather this band is ascribable to polaron pairs of RRa-P3HT, as will be described below.

2.1.2. Intensity Dependence of Transient Signals at 0 ps. To distinguish the two absorption bands at around 700 and 1000 nm, we measured the initial transient signals at 0 ps under different excitation intensities at 400 nm. Note that the transient absorption at 650 nm is plotted instead of that at 700 nm to minimize the spectral overlap of the singlet exciton band at an early time stage. As shown in Figure 4, the initial transient signal at 1000 nm increased linearly with increasing excitation intensity under lower intensities, <30 μJ cm^{-2}, which corresponds to photon densities of $< 7 \times 10^{18}$ cm^{-3}, and increased sublinearly with an exponent $\alpha \approx 0.5$ of the power-law equation $\Delta OD \propto I^{\alpha}$ under higher intensities, >30 μJ cm^{-2}. On the contrary, the exponent of the power-law equation for the transient signal at 650 nm changed from 1 (<30 μJ cm^{-2}) to $\sim$1.4 (>30 μJ cm^{-2}), which was a threshold similar to that of the transient signal at 1000 nm. The different intensity dependences indicate that the two bands originate from different transient species, which is consistent with the assignment mentioned above. The smaller exponent of $\sim$0.5 observed for the transient signal at 1000 nm suggests that a bimolecular reaction dominates the deactivation of singlet excitons,[21] which is mainly attributed to singlet exciton−exciton annihilation on a time scale shorter than the excitation pulse width (<100 fs) under higher intensities. Such a rapid annihilation suggests that the average distance between two excitons is smaller than the annihilation radius at higher intensities, because exciton migration is negligible on such a short time scale. On the other hand, the larger exponent of $\sim$1.4 observed for the transient signal at 650 nm indicates that polaron pairs are more efficiently formed at higher excitation intensities, which is related to the rapid singlet exciton−exciton annihilation.

2.1.3. Anisotropy Decays. To clarify the dynamics of polaron pairs and singlet excitons, we measured time-dependent anisotropy decays of the two characteristic absorption bands at 700 and 1000 nm at lower intensities, <30 μJ cm^{-2}, where the rapid singlet exciton−exciton annihilation was negligible at 0 ps. Upon the excitation at 400 nm, as shown in Figure 5, the anisotropy at 700 nm was as large as $r \approx 0.35$ immediately after the laser excitation, was reduced to $r \approx 0.25$ after a few picoseconds, and remained constant at $r \approx 0.25$ up to the nanosecond time domain. On the other hand, the anisotropy at 1000 nm was as small as $r < 0.1$ at 0 ps and negligible, $r \approx 0$, a few picoseconds after the laser excitation. This distinct difference is again consistent with our assignment that the 700

(21) Watanabe, S.; Furube, A.; Katoh, R. *J. Phys. Chem. A* **2006**, *110*, 10173–10178.

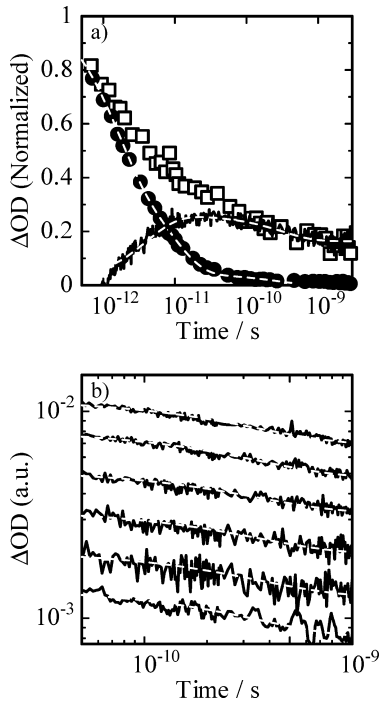

Figure 6. (a) Normalized femtosecond transient absorption decays of RRa-P3HT films excited at 400 nm (~30 μJ cm^{-2}) measured at 1000 nm (closed circles) and 825 nm (open squares). The solid line shows the rise fraction at 825 nm that is evaluated by subtracting the transient absorption signal at 1000 nm from that at 825 nm. The transient absorption decay at 1000 nm was fitted with a sum of three exponential functions: $\Delta OD(t) = A_{D1} \exp(-t/\tau_{D1}) + A_{D2} \exp(-t/\tau_{D2}) + A_{D3} \exp(-t/\tau_{D3})$. The subtracted transient absorption signal at 825 nm was fitted with an exponential function: $\Delta OD(t) = -A_R \exp(-t/\tau_R) + A_D \exp(-t/\tau_D) + B$. The broken lines represent the best fitting curves. (b) Femtosecond transient absorption decays at 825 nm with different fluences of 6, 12, 24, 48, 72, and 120 μJ cm^{-2} from bottom to top. The decays were fitted with an exponential equation: $\Delta OD(t) = A_D \exp(-t/\tau_D) + B$. The broken lines represent the best fitting curves.

nm band is ascribed to neither singlet nor triplet excitons but polaron pairs. The small anisotropy at 0 ps suggests that the polarization memory of singlet excitons rapidly disappears within the laser excitation (~100 fs), which is comparable to the vibrational relaxation. The rapid decrease in the anisotropy suggests that there is an efficient relaxation pathway of singlet excitons to change the polarization direction. On the other hand, the large anisotropy observed at 700 nm indicates that the formation of polaron pairs is in competition with such a rapid relaxation of singlet excitons on a time scale less than 100 fs. Furthermore, the anisotropy at 700 nm was as large as $r \approx 0.25$ up to the nanosecond time domain, suggesting that it cannot be assigned to freely mobile species, which is also consistent with our assignment of the 700 nm band to polaron pairs. Upon the excitation at 500 nm, on the other hand, the anisotropy at 1000 nm was as large as $r \approx 0.4$ immediately after the laser excitation and decayed to $r \approx 0.05$ with a time constant of ~4 ps. The difference in the initial anisotropy indicates that the initial relaxation of singlet excitons depends upon the excitation wavelength as will be discussed later.

2.1.4. Transient Absorption Decays. We measured transient absorption decays at 1000 and 825 nm to discuss the decay and formation dynamics of singlet and triplet excitons after the 400 nm excitation. For singlet excitons, as shown in Figure 6a, the transient absorption decay at 1000 nm was fitted with a sum of three exponential functions under an excitation intensity of 30 μJ cm^{-2}: $\Delta OD(t) = A_{D1} \exp(-t/\tau_{D1}) + A_{D2} \exp(-t/\tau_{D2}) + A_{D3} \exp(-t/\tau_{D3})$. The longest lifetime, τ_{D3}, was fixed to a photoluminescence lifetime of 270 ps, which was evaluated by the time-correlated single photon counting (TCSPC) measurement where the excitation intensity was as low as ~nJ cm^{-2}. The remaining two lifetimes shortened with increasing excitation intensity. The averaged shorter lifetime (4.5 ps) is therefore ascribed to an efficient deactivation of singlet excitons due to the singlet exciton−exciton annihilation. In this time domain, the exciton−exciton annihilation probably results from the efficient exciton migration in RRa-P3HT films. For triplet excitons, as shown in Figure 6a, the formation dynamics of triplet excitons was deduced by subtracting the decay fraction of singlet excitons from the transient absorption decay at 825 nm, because a large absorption tail of singlet excitons was dominant at an early time stage although triplet excitons exhibited an absorption peak at 825 nm. Note that triplet formation at 0 ps was negligible, because no distinct triplet signal was observed at this low excitation intensity, which is generally consistent with the slow intersystem crossing (ISC) rate of conjugated polymers. The deduced decay can be fitted with a rise time constant of 4.0 ps and a decay time constant of 320 ps with a long-lived constant fraction. The coincidence between the decay time constant of singlet excitons (4.5 ps) and the rise time constant of triplet excitons (4.0 ps) strongly suggests that triplet excitons are interconverted from singlet excitons. However, this interconversion time, ~4 ps, is too fast to be assigned to ISC from the lowest singlet exciton state. The ISC rate has been reported to be ~1 ns^{-1} for poly(3-octylthiophene) in a xylene solution.[22] Furthermore, as shown in Figure 6b, the triplet exciton band at 825 nm decayed on a subnanosecond time scale. This lifetime is also too short to be assigned to "isolated" triplet excitons, which should decay with a lifetime of several microseconds as shown in the inset of Figure 2. The short lifetime cannot be ascribed to bimolecular deactivation such as triplet exciton−exciton annihilation, because the decay dynamics was independent of the excitation intensity. We will discuss the rapid formation and decay of triplet excitons later.

2.2. RR-P3HT. 2.2.1. Transient Absorption Spectra. Turning now to a more crystalline polymer, RR-P3HT (see the Supporting Information), transient absorption spectra were slightly different from those of amorphous RRa-P3HT films. Parts a−d of Figure 7 show transient absorption spectra of RR-P3HT films excited at 400 nm under different excitation intensities measured from 0 to 3 ns. At lower excitation intensities (<15 μJ cm^{-2}), a large absorption band was observed at around 1200 nm, which was red-shifted to 1250 nm at 100 ps, and a small absorption band was observed at around 650 nm immediately after the laser excitation. Both bands decayed rapidly on the picosecond time scale, and a relatively long-lived absorption band was observed at around 1000 nm at a later time stage. At higher excitation intensities (>15 μJ cm^{-2}), the 1200 nm band decayed more rapidly, and instead the 1000 nm band was mainly observed along with a more distinct absorption band at around 650 nm immediately after the laser excitation. In other words, with increasing excitation intensity, the absorption at 1200 nm decreased whereas the absorption bands at 650 and 1000 nm increased. The absorption band at around 1200 nm observed immediately after the laser excitation can be ascribed to singlet excitons of RR-P3HT, because it had a decay constant similar to the photoluminescence lifetime (~ 330 ps) of the RR-P3HT

(22) Kraabel, B.; Moses, D.; Heeger, A. J. *J. Chem. Phys.* **1995**, *103*, 5102–5108.

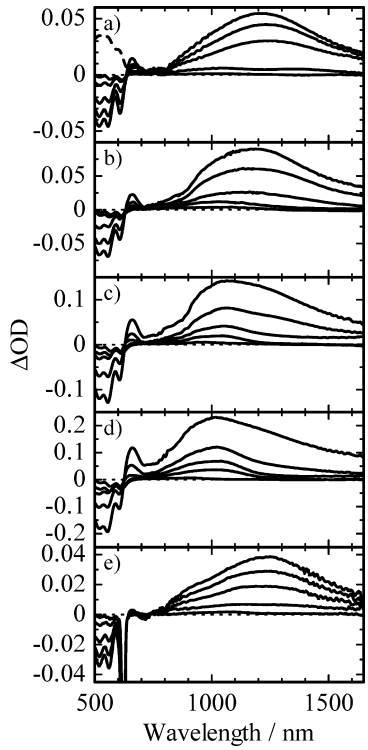

Figure 7. Femtosecond transient absorption spectra of RR-P3HT films measured at a delay time of 0, 1, 10, 100, and 3000 ps from top to bottom in each panel. The excitation intensity was varied as follows: (a) 15 μJ cm^{-2}, (b) 30 μJ cm^{-2}, (c) 60 μJ cm^{-2}, (d) 120 μJ cm^{-2}, (e) 10 μJ cm^{-2}. The excitation wavelengths were (a−d) 400 nm and (e) 620 nm. The broken line represents the steady-state absorption spectrum of the RR-P3HT film.

film under lower excitation intensities as mentioned later. This assignment is in agreement with previous reports although the peak wavelength was substantially longer than those reported.[12,13,23] The absorption band at around 1000 nm had the longest lifetime but disappeared on the nanosecond scale, which is too short to be assigned to triplet excitons. Indeed, no long-lived transients were observed on the microsecond time scale, which corresponds to the lifetime of triplet excitons in various thiophene-based polymers including RRa-P3HT.[24,25] This absorption band is consistent with that reported for intrachain polarons in RR-P3HT films observed by steady-state photomodulation spectroscopy[12−14,19] and also for trapped polarons in a blend film of RR-P3HT and a fullerene derivative observed by transient absorption spectroscopy.[25] Therefore, the absorption band observed at 1000 nm is attributed to polarons of RR-P3HT. On the other hand, the absorption band at around 650 nm is ascribed to polaron pairs of RR-P3HT, because the decay dynamics was independent of the excitation intensity as is described below, which is consistent with previous reports.[12,13] Upon the excitation at 620 nm, as shown in Figure 7e, the singlet exciton band was observed at around 1250 nm but no absorption of polaron pairs was observed at around 650 nm immediately after the laser excitation. The singlet exciton band at 1250 nm

(23) Hwang, I.-W.; Moses, D.; Heeger, A. J. *J. Phys. Chem. C* **2008**, *112*, 4350–4354.
(24) Ohkita, H.; Cook, S.; Astuti, Y.; Duffy, W.; Heeney, M.; Tierney, S.; McCulloch, I.; Bradley, D. D. C.; Durrant, J. R. *Chem. Commun.* **2006**, *37*, 3939–3941.
(25) Ohkita, H.; Cook, S.; Astuti, Y.; Duffy, W.; Tierney, S.; Zhang, W.; Heeney, M.; McCulloch, I.; Nelson, J.; Bradley, D. D. C.; Durrant, J. R. *J. Am. Chem. Soc.* **2008**, *130*, 3030–3042.

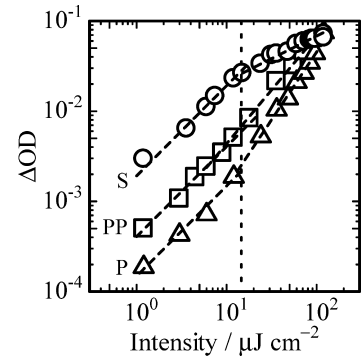

Figure 8. Log−log plots of the initial transient signals of RR-P3HT films at 1200 nm (singlet exciton, S; open circles), 660 nm (polaron pair, PP; open squares), and 1000 nm (polaron, P; open triangles) against the excitation intensity. The broken lines represent fitting curves with a power-law equation: $\Delta OD \propto I^{\alpha}$. The dotted line exhibits the turning point from linear to nonlinear dependence of the transient signals ($\sim$15 μJ cm^{-2}).

decayed with no peak shift on the picosecond time scale. Similarly to the 400 nm excitation, a relatively long-lived absorption band was also observed at around 1000 nm at a later time stage.

2.2.2. Intensity Dependence of Transient Signals at 0 ps. To study the ultrafast formation dynamics of the three transient species, singlet excitons, polarons, and polaron pairs, we evaluated the initial transient signals at 0 ps under different excitation intensities. Each contribution of singlet excitons and polarons was evaluated by spectral analysis of the transient spectra at 0 ps. Details of the spectral analysis are given in the Supporting Information. Figure 8 shows log−log plots of each transient signal against various excitation intensities at 400 nm. Under lower excitation intensities, <15 μJ cm^{-2}, which correspond to photon densities of $<3 \times 10^{18}$ cm^{-3}, all three transient signals exhibited a linear dependence with a slope of almost unity, $\alpha \approx 1$, in the power-law equation $\Delta OD \propto I^{\alpha}$. Under higher excitation intensities, >15 μJ cm^{-2}, the slope was $\sim$0.5 for the transient signal at 1200 nm whereas it was $\sim$1.2 at 660 nm and $\sim$1.5 at 1000 nm. The sublinear dependence of the singlet exciton band at 1200 nm suggests that the singlet exciton−exciton annihilation dominates the deactivation of singlet excitons on a time scale less than the excitation pulse width (<100 fs) under higher excitation intensities. On the other hand, the superlinear dependence of the polaron pair band at 660 nm and the polaron band at 1000 nm indicates that there is another pathway for the generation of polaron pairs and polarons at higher excitation intensities, which is probably related to the singlet exciton−exciton annihilation because the turning point was observed at a similar excitation intensity ($\sim$15 μJ cm^{-2}).

Figure 9 shows the absorbance ratio of the polaron fraction to the singlet exciton fraction that was evaluated by the spectral division with two separated peaks. For the 400 nm excitation, the ratio was nearly a constant value of $\sim$0.06 under lower photon densities, $<3 \times 10^{18}$ cm^{-3}, and increased monotonically under higher photon densities, $>3 \times 10^{18}$ cm^{-3}. For the 620 nm excitation, on the other hand, the ratio was negligible under lower photon densities, $<8 \times 10^{17}$ cm^{-3}, and increased monotonically under higher photon densities, $>8 \times 10^{17}$ cm^{-3}. The higher absorbance ratio observed at higher photon densities indicates that the polaron generation is due to the singlet exciton−exciton annihilation. Interestingly, the ratio for the 620 nm excitation started to increase at a lower photon density (8×10^{17} cm^{-3}) compared to that for the 400 nm excitation (3×10^{18} cm^{-3}), suggesting that the singlet exciton−exciton an-

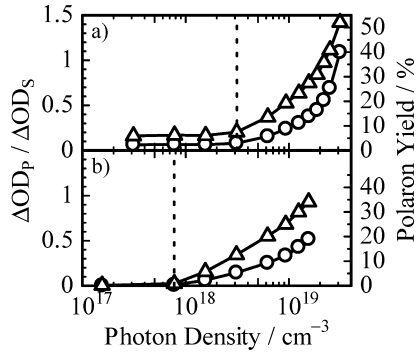

Figure 9. Initial absorption ratio of polarons to singlet excitons (open circles) in RR-P3HT films plotted against the photon density excited at (a) 400 nm and (b) 620 nm. The right axis of this figure shows the initial polaron yields ($\Delta OD_P/(\Delta OD_P + \Delta OD_S)$, open triangles) based on an assumption of $\varepsilon_{P(1000nm)}/\varepsilon_{S(1200nm)} \approx 1$.[17] The dotted lines exhibit the turning points of the polaron yields: 3×10^{18} cm^{-3} for the 400 nm excitation and 8×10^{17} cm^{-3} for the 620 nm excitation.

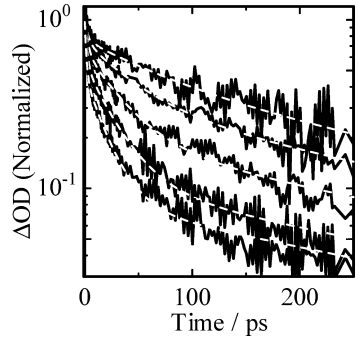

Figure 10. Normalized transient absorption decays of RR-P3HT films excited at 400 nm measured at 1200 nm. The excitation intensity was varied over 1.2, 3, 6, 12, and 24 μJ cm^{-2} from top to bottom. The broken lines represent fitting curves with a sum of three exponential functions: $\Delta OD(t) = A_{D1} \exp(-t/\tau_{D1}) + A_{D2} \exp(-t/\tau_{D2}) + A_{D3} \exp(-t/\tau_{D3})$.

nihilation would occur more efficiently upon the excitation at 620 nm. We will discuss the formation dynamics and yield of polarons later.

2.2.3. Transient Absorption Decays. We measured the transient absorption decays under different excitation intensities to discuss the decay dynamics of the three transient species, singlet excitons (1200 nm), polarons (1000 nm), and polaron pairs (660 nm) after the 400 nm excitation. First, as shown in Figure 10, the transient absorption at 1200 nm ascribed to singlet excitons decayed faster under higher excitation intensities, which was fitted with a sum of three exponential functions as summarized in Table 1: $\Delta OD(t) = A_{D1} \exp(-t/\tau_{D1}) + A_{D2} \exp(-t/\tau_{D2}) + A_{D3} \exp(-t/\tau_{D3})$. The longest lifetime, τ_{D3}, was fixed for all the excitation intensities to a photoluminescence lifetime of 330 ps, which was evaluated by the TCSPC measurement. With increasing excitation intensity, the fraction of the longest lifetime decreased and the remaining lifetimes shortened. This intensity dependence of the decay dynamics indicates that the singlet exciton is deactivated dominantly by the singlet exciton−exciton annihilation at higher excitation intensities. Second, as shown in Figure 11a, the transient absorption decays at 1000 nm ascribed to polarons depended upon the excitation intensity. Note that neither singlet excitons nor polaron pairs contributed to the absorption in the nanosecond time domain because of their shorter lifetimes. At higher excitation intensities (>6 μJ cm^{-2}), the transient signal decayed faster with the intensity, indicating that bimolecular recombination is dominant. In other words,

Table 1. Fitting Parameters for Transient Absorption Decays of RR-P3HT Films at 1200 nm[a]

intensity/μJ cm^{-2}	$A_{D1,2,av}$/%	$\tau_{D1,2,av}$/ps	A_{D3}/%	τ_{D3}/ps
1	57	26	43	330
3	70	21	30	330
6	81	17	19	330
12	89	13	11	330
24	92	8	8	330

[a] Transient absorption decays at 1200 nm were fitted with a sum of three exponential functions: $\Delta OD(t) = A_{D1} \exp(-t/\tau_{D1}) + A_{D2} \exp(-t/\tau_{D2}) + A_{D3} \exp(-t/\tau_{D3})$. The longest lifetime, τ_{D3}, was fixed to a photoluminescence lifetime of 330 ps for all excitation intensities. The fraction $A_{D1,2,av}$ and the lifetime $\tau_{D1,2,av}$ represent the total fraction of A_{D1} and A_{D2} and the averaged lifetime between τ_{D1} and τ_{D1}, respectively.

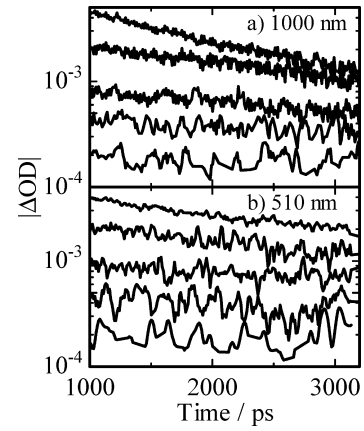

Figure 11. Femtosecond transient absorption decays of RR-P3HT films excited at 400 nm measured at (a) 1000 nm and (b) 510 nm. The excitation intensity was varied over 1.2, 6, 12, 36, and 120 μJ cm^{-2} from bottom to top. The negative transient signals at 510 nm are converted to positive.

polarons would recombine with other polarons bimolecularly, suggesting that they can migrate freely in the nanosecond time domain. In parallel with the intensity-dependent decay dynamics of polarons, the photobleaching signal at 510 nm, which is due to the ground-state depletion, was also dependent upon the excitation intensity as shown in Figure 11b. This coincidence suggests that the decay of polarons can be ascribed to bimolecular recombination, leading to the ground state. At lower excitation intensities (<6 μJ cm^{-2}), on the other hand, the transient signal at 1000 nm remained almost constant, which was also consistent with the photobleaching signal at 510 nm. Interestingly, the remaining constant signal at 1000 nm was the same as the initial signal at 0 ps shown in Figure 8, suggesting that most of the polarons are generated immediately after the laser excitation and free from the bimolecular recombination up to the nanosecond time domain. Third, as shown in Figure 12a, the transient signal decays at 660 nm ascribed to polaron pairs were independent of the excitation intensity in contrast to the decay dynamics at 1200 and 1000 nm. The transient absorption decays were fitted with a monoexponential function with a lifetime of ~0.8 ps (~80%) and a constant fraction (~20%) over the whole excitation intensity measured as summarized in Table 2. The intensity-independent decay at 660 nm in several picoseconds suggests that the decay dynamics of polaron pairs is dominated by a monomolecular process such as geminate recombination. On the other hand, Figure 12b shows transient absorption decays at 510 nm that are ascribable to the photobleaching signal. The decay dynamics at 510 nm was also fitted with a monoexponential function and a constant fraction. However, the monoexponential lifetime at 510 nm was different

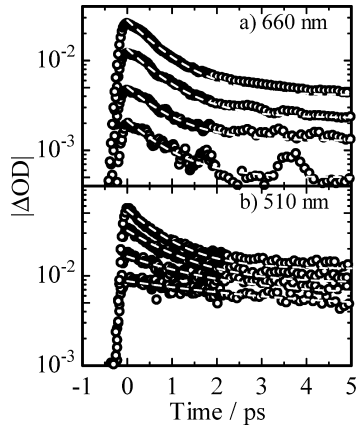

Figure 12. Femtosecond transient absorption decays of RR-P3HT films excited at 400 nm measured at (a) 660 nm and (b) 510 nm. The excitation intensity was varied over 15, 30, 60, and 120 μJ cm^{-2} from bottom to top. The negative transient signals at 510 nm are converted to positive. The broken lines represent fitting curves with an exponential function and a constant fraction: $\Delta OD(t) = A_D \exp(-t/\tau_D) + B$.

Table 2. Fitting Parameters for Transient Absorption Decays of RR-P3HT Films at 660 and 510 nm[a]

	660 nm			510 nm		
intensity/μJ cm^{-2}	A_D/%	τ_D/ps	B/%	A_D/%	τ_D/ps	B/%
15	83	0.8	17	52	3.1	48
30	78	0.8	22	63	1.7	37
60	83	0.9	17	74	1.1	26
120	85	0.9	15	78	0.8	22

[a] Transient absorption decays at 660 and 510 nm were fitted with an exponential function and a constant fraction: $\Delta OD(t) = A_D \exp(-t/\tau_D) + B$.

from that at 660 nm, and with increasing excitation intensity the lifetime shortened and the decay fraction increased in contrast to the decay dynamics at 660 nm. Note that the faster decay at 510 nm observed at higher intensities is ascribable to the singlet exciton−exciton annihilation because it was in agreement with the decay of singlet excitons at 1200 nm. Therefore, this disagreement suggests that polaron pairs in RR-P3HT films do not recombine to the ground state on the picosecond time scale as will be discussed later.

3. Discussion

3.1. Assignments of Transient Species. We first summarize the assignments of transient species observed for RRa-P3HT and RR-P3HT pristine films before discussing the photophysics in the films in detail. For RRa-P3HT, we observed three characteristic absorption bands at around 700, 800, and 1000 nm, which are ascribed to polaron pairs, triplet excitons, and singlet excitons, respectively. For RR-P3HT, we observed three characteristic absorption bands at around 650, 1000, and 1200 nm, which are ascribed to polaron pairs, polarons, and singlet excitons, respectively. To singlet excitons we safely assign the absorption bands at 1000 nm (RRa-P3HT) and at 1200 nm (RR-P3HT), because both bands were observed immediately after the laser excitation and decayed with the same time constant as that of the photoluminescence. As shown in Figures 1 and 7, the transient absorption band was red-shifted with time from 900 to 1060 nm for RRa-P3HT and from 1200 to 1250 nm for RR-P3HT, which is indicative of the delocalization of singlet excitons. The difference in the peak wavelength suggests that singlet excitons are more delocalized in RR-P3HT than in RRa-P3HT not only immediately after the laser excitation but also at the final stage, which is consistent with previous reports.[12,13] To triplet excitons we safely assign the absorption band at 800 nm (RRa-P3HT), because this band decayed monomolecularly with a lifetime of 7 μs and was quenched under an O_2 atmosphere. Note that on a subnanosecond time scale the triplet exciton band at 825 nm as shown in Figure 6b is ascribed not to isolated triplet excitons but to triplet exciton pairs as will be discussed later. To polaron pairs we assign the absorption bands at 700 nm (RRa-P3HT) and at 650 nm (RR-P3HT), because both bands were observed immediately after the laser excitation at 400 nm and decayed monomolecularly but were not observed upon the excitation close to the band gap. The anisotropy results also support this assignment. The absorption band was blue-shifted with respect to that of polarons. The Coulomb attraction between the oppositely charged polaron pairs formed on adjacent chains is considered to cause such blue-shifted absorption,[26,27] while it is negligible between free polarons. The polaron pair band of the RR-P3HT film was slightly blue-shifted in comparison with that of the RRa-P3HT film. The blue-shifted absorption might be due to a shorter electron−hole separation of polaron pairs on adjacent chains in the RR-P3HT crystalline domain rather than in the RRa-P3HT amorphous domain. To polarons we assign the absorption band at 1000 nm (RR-P3HT), because the lifetime is too long to be assigned to singlet excitons or polaron pairs and too short to be assigned to isolated triplet excitons. The possibility of triplet exciton pairs as mentioned above also can be ruled out because the decay dynamics was dependent upon the excitation intensity, suggesting bimolecular recombination. Furthermore, the spectrum is consistent with previous reports.[13,14,28] In general, polarons have two absorption bands: a transition from the HOMO to the SOMO (P_1 transition) and a transition from the SOMO to the LUMO (P_2 transition). The 1000 nm band corresponds to the P_2 transition.

These assignments are almost consistent with previous reports, but there are several discrepancies. The most remarkable difference is the observation of the ultrafast triplet formation in RRa-P3HT films. In previous reports, no triplet formation has been reported on the picosecond time scale. We will discuss the formation mechanism later in detail. Another discrepancy is the difference in the peak wavelength of the singlet exciton band. For RRa-P3HT, we observed the absorption band of singlet excitons at around 1000 nm while it is reported to be observed at 885 nm in previous reports.[12,13] For RR-P3HT, we observed the absorption band of singlet excitons at around 1200 nm while it is reported to be at 950 nm[12,13] and at 1000 nm.[23] We should note that the transient absorption spectra on the picosecond time scale depended upon the excitation intensity especially in RR-P3HT. As shown in Figure 7, the absorption band of singlet excitons at around 1200 nm disappeared at higher excitation intensities because of the singlet exciton−exciton annihilation. Instead the absorption band of polarons became pronounced at around 1000 nm. A typical photon flux of our femtosecond laser pulse (400 nm, 10 μJ cm^{-2}, ~100 fs) is estimated to be ~2×10^{26} photons cm^{-2} s^{-1} (10^8 W cm^{-2}), which is relatively lower than that reported previously. Recently Cook and his co-workers have reported the absorption band of singlet excitons at around 1250 nm for RR-P3HT films,[19] which

(26) Lane, P. A.; Wei, X.; Vardeny, Z. V. *Phys. Rev. B* **1997**, *56*, 4626–4637.
(27) Mizes, H. A.; Conwell, E. M. *Phys. Rev. B* **1994**, *50*, 11243–11246.
(28) Beljonne, D.; Cornil, J.; Sirringhaus, H.; Brown, P. J.; Shkunov, M.; Friend, R. H.; Brédas, J.-L. *Adv. Funct. Mater.* **2001**, *11*, 229–234.

is in good agreement with our observation. They also employed a relatively low excitation pulse ($\sim 2 \times 10^{25}$ photons cm^{-2} s^{-1}) from a subnanosecond Nd:YAG laser. Therefore, we note that the absorption band at around 1000 nm reported for RR-P3HT films previously should be mainly assigned to polarons rather than singlet excitons.

3.2. Singlet Exciton Delocalization. Before discussing the delocalization of singlet excitons, we focus our attention on the rapid relaxation of singlet excitons in RRa-P3HT films during the excitation pulse of 100 fs. As shown in Figure 5b, the anisotropy for the singlet exciton band observed at 1000 nm was as small as $r < 0.1$ even at 0 ps immediately after the laser excitation at 400 nm, suggesting that there is a rapid relaxation pathway within 100 fs to reduce the anisotropy. Such a rapid anisotropy decay of singlet excitons has been reported for conjugated polymers such as poly(*p*-phenylenevinylene) and polythiophene derivatives, which is ascribed to the dynamic localization of the singlet exciton (exciton self-trapping) as rapid as <100 fs.[29−34] The high-energy excitation is likely to produce unstable singlet excitons along twisted segments, which are considered to be rapidly localized at one segment in the dynamic localization driven by structural relaxation of excited segments.[32] Indeed, upon the low-energy excitation the anisotropy for the singlet exciton band was as large as $r \approx 0.4$ at 0 ps immediately after the laser excitation at 500 nm, which can selectively excite longer conjugated segments to generate more stable singlet excitons. Therefore, we ascribe the rapid relaxation of singlet excitons to the dynamic localization.

We next move onto the delocalization of singlet excitons on the picosecond time scale. For RRa-P3HT, as shown in Figure 1, the singlet exciton band was red-shifted with time from 900 to 1060 nm ($\Delta E \approx 0.21$ eV) for the 400 nm excitation and from 1000 to 1060 nm ($\Delta E \approx 0.07$ eV) for the 500 nm excitation. On the other hand, the anisotropy of the singlet exciton band decayed with a time constant of ~4 ps upon the 500 nm excitation, which was consistent with the decay time constant of the singlet excitons under the bimolecular annihilation as mentioned above. These results therefore suggest that singlet excitons efficiently migrate on the picosecond time scale, resulting in the singlet−singlet exciton annihilation and the exciton delocalization into longer conjugated segments. For RR-P3HT, as shown in Figure 7, the singlet exciton band was red-shifted with time from 1200 to 1250 nm ($\Delta E \approx 0.04$ eV) for the 400 nm excitation and already observed at 1250 nm immediately after the laser excitation at 620 nm. This difference suggests that the exciton delocalization dynamics is dependent upon the excitation wavelength. As shown in Figure 9, the 400 nm excitation gave a higher threshold intensity for the polaron formation (3×10^{18} cm^{-3}) than the 620 nm excitation (8×10^{17} cm^{-3}), suggesting that the interaction radius between singlet excitons is also dependent upon the excitation wavelength. An averaged interaction radius of two excitons in RR-P3HT at 0 ps is quantitatively estimated to be ~4.3 nm for the 400 nm excitation whereas ~6.7 nm for the 620 nm excitation from the threshold of the photon density. From the threshold intensity of 7×10^{18} cm^{-3}, the interaction radius of singlet excitons in RRa-P3HT films is estimated to be ~3.2 nm at 0 ps after the 400 nm excitation. There are three possible explanations for the different interaction radius between RRa-P3HT and RR-P3HT: (1) dipole−dipole interaction of excitons due to Förster energy transfer,[35−37] (2) exciton migration,[36] and (3) exciton delocalization.[38] The dipole−dipole interaction of singlet excitons and the exciton migration are negligible on a time scale shorter than the excitation pulse width (<100 fs). Therefore, we conclude that the long-range interaction of singlet excitons at 0 ps is due to the exciton delocalization. These results show that singlet excitons are delocalized over the interaction radius at 0 ps: ~4.3 nm (~11 repeating units) for the 400 nm excitation and ~6.7 nm (~17 repeating units) for 620 nm excitation in RR-P3HT and ~3.2 nm (~8 repeating units) in RRa-P3HT, which are roughly consistent with the order of the exciton delocalization for conjugated polymers by quantum calculations.[39] In other words, singlet excitons are more delocalized in RR-P3HT films than in RRa-P3HT films, which is consistent with the peak wavelengths of the singlet exciton band as discussed above. Note that the interaction radii of singlet excitons in P3HTs are estimated as a three-dimensional sphere without taking their anisotropic distribution into consideration.

3.3. Polaron Pair Formation. Here we discuss the important findings on the formation of polaron pairs in RRa-P3HT films. For the 400 nm excitation, as shown in Figure 1, the 700 nm band ascribed to polaron pairs was observed immediately after the laser excitation. The transient signal at 0 ps superlinearly increased with increasing excitation intensity, whereas the singlet exciton band at 1000 nm sublinearly increased (>30 μJ cm^{-2}). Furthermore, the anisotropy for the polaron pair band at 700 nm was as large as $r \approx 0.35$ at 0 ps and remained constant at $r \approx 0.25$ up to the nanosecond time domain, whereas that for the singlet exciton band at 1000 nm was as small as $r < 0.1$ even at 0 ps because of the dynamic localization. These results suggest that polaron pairs are generated from nonrelaxed exciton states in competition with rapid vibrational relaxations such as the dynamic localization of the singlet exciton and cannot migrate freely but are rather tightly bound as geminate ion pairs. The same holds true for polaron pairs in RR-P3HT films because the prompt formation of polaron pairs was observed at 0 ps as shown in Figure 7. Such a rapid formation of polaron pairs can be explained by the hot-exciton dissociation model in conjugated polymers.[40−42] The main idea of this model is that the excess energy of the excitation photon is quickly distributed over the conjugation segment of the chain, resulting in a high effective temperature. The exciton has a chance to dissociate as long as the effective temperature is high enough to provide the activation energy. Thus, the threshold of excess photon energy for the

(29) Dykstra, T. E.; Kovalevskij, V.; Yang, X.; Scholes, G. D. *Chem. Phys.* **2005**, *318*, 21–32.
(30) Grage, M. M.-L.; Zaushitsyn, Y.; Yartsev, A.; Chachisvilis, M.; Sundström, V.; Pullerits, T. *Phys. Rev. B* **2003**, *67*, 205207.
(31) Yang, X.; Dykstra, T. E.; Scholes, G. D. *Phys. Rev. B* **2005**, *71*, 045203.
(32) Ruseckas, A.; Wood, P.; Samuel, I. D. W.; Webster, G. R.; Mitchell, W. J.; Burn, P. L.; Sundström, V. *Phys. Rev. B* **2005**, *72*, 115214.
(33) Gaab, K. M.; Bardeen, C. J. *J. Phys. Chem.* **2004**, *108*, 4619–4626.
(34) Scheblykin, I. G.; Yartsev, A.; Pullerits, T.; Gulbinas, V.; Sundström, V. *J. Phys. Chem. B* **2007**, *111*, 6303–6321.
(35) Westenhoff, S.; Daniel, C.; Friend, R. H.; Silva, C.; Sundström, V.; Yartsev, A. *J. Chem. Phys.* **2005**, *122*, 094903.
(36) Stevens, M. A.; Silva, C.; Russell, D. M.; Friend, R. H. *Phys. Rev. B* **2001**, *63*, 165213.
(37) Wells, N. P.; Boudouris, B. W.; Hillmyer, M. A.; Blank, D. A. *J. Phys. Chem. C* **2007**, *111*, 15404–15414.
(38) Dogariu, A.; Vacar, D.; Heeger, A. J. *Phys. Rev. B* **1998**, *58*, 10218–10224.
(39) Köhler, A.; dos Santos, D. A.; Beljonne, D.; Shuai, Z.; Brédas, J.-L.; Holmes, A. B.; Kraus, A.; Müllen, K.; Friend, R. H. *Nature* **1998**, *392*, 903–906.
(40) Arkhipov, V. I.; Emelianova, E. V.; Bässler, H. *Phys. Rev. Lett.* **1999**, *82*, 1321–1324.
(41) Arkhipov, V. I.; Emelianova, E. V.; Barth, S.; Bässler, H. *Phys. Rev. B* **2000**, *61*, 8207–8214.
(42) Basko, D. M.; Conwell, E. M. *Phys. Rev. B* **2002**, *66*, 155210.

Scheme 1. Energy Diagram for Polaron Pair and Polaron Formation in RR-P3HT Films[a]

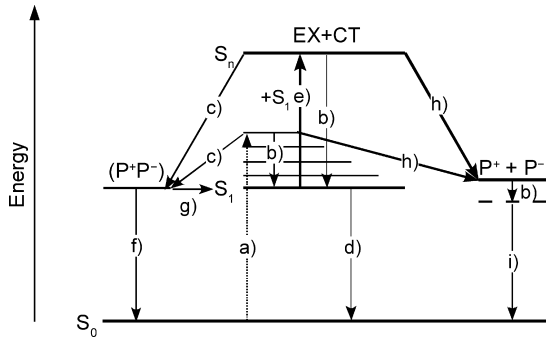

[a] Key: (a) photon absorption, (b) vibrational relaxation, (c) polaron pair formation, (d) monomolecular deactivation (k_F, k_N, and k_{ISC}), (e) singlet exciton−exciton annihilation (singlet fusion), (f) geminate recombination to the ground state, (g) geminate recombination to the singlet exciton state, (h) polaron formation, (i) bimolecular recombination.

Scheme 2. Energy Diagram for Polaron Pair and Triplet Exciton Formation in RRa-P3HT Films[a]

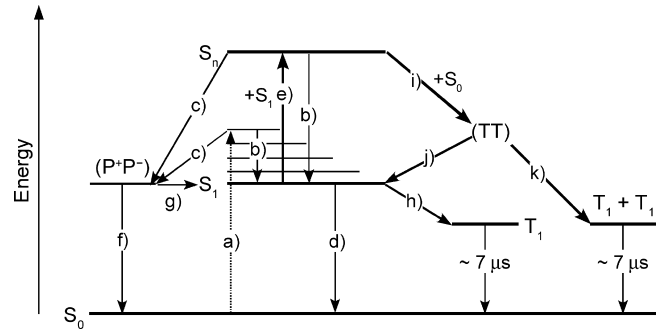

[a] Key: (a) photon absorption, (b) vibrational relaxation, (c) polaron pair formation, (d) radiative and nonradiative deactivations (k_F, k_N), (e) singlet exciton−exciton annihilation (singlet fusion), (f) geminate recombination to the ground state, (g) geminate recombination to the singlet exciton state, (h) intersystem crossing (k_{ISC}), (i) singlet fission, (j) triplet fusion, (k) triplet pair dissociation.

polaron pair generation is considered to be closely related to the exciton binding energy, which has been reported to be ~0.5 eV for various conjugated polymers.[43] Indeed, as shown in Figure 1, no polaron pairs were observed after the laser excitation at 500 nm close to the band gap of RRa-P3HT. Furthermore, the photocurrent has been reported to increase strongly at excitation energies about 1 eV above the absorption edge.[39] In this model, the rate of the hot-exciton dissociation by the photon absorption has been estimated to be less than 100 fs for conjugated polymers even in the absence of an electric field. In our experiment, the excess energy is as large as 0.8 eV for one photon excitation by the 400 nm laser pulse and 2.3 eV for a higher excitation by the singlet exciton−exciton annihilation. Either excess energy is much larger than the exciton binding energy and therefore can cause the polaron pair formation in competition with rapid vibrational relaxations along with the dynamic localization as mentioned before. In particular, geminate polaron pairs are likely to be more efficiently formed from higher exciton states than from the lowest exciton state, because theoretical calculations predict that higher exciton states are more mixed with interchain charge transfer (CT) states so that electron and hole pairs are formed on adjacent chains.[44] We therefore conclude that geminate polaron pairs are generated, in competition with the vibrational relaxation, from a higher vibrational state in the lowest singlet exciton state under lower excitation intensities, and additionally from a higher singlet exciton state produced by the singlet exciton−exciton annihilation under higher excitation intensities as shown in Schemes 1 and 2.

In comparison with RRa-P3HT, RR-P3HT exhibited a more distinct absorption band of polaron pairs in the visible region upon excitation at 400 nm, suggesting that the formation yield of polaron pairs is more efficient in RR-P3HT films. This can be explained in terms of the hot-exciton dissociation mentioned above. The hot exciton formed in RR-P3HT has a larger excess energy than that formed in RRa-P3HT because of the smaller band gap in RR-P3HT, which may result in more efficient formation of polaron pairs. Considering the different film morphologies, on the other hand, the larger interchain interaction in crystalline RR-P3HT films is likely to cause the larger mixing of interchain CT configurations. Exciton states containing significant weights of CT configurations are known as CT excitons, which are considered to play an important role in photoconduction or photocurrent generation of charge carriers.[44] Therefore, the larger mixing of interchain CT configurations also can account for the more efficient formation of polaron pairs in RR-P3HT. We speculate that CT excitons formed in RR-P3HT films can partly dissociate into polarons in competition with the formation of polaron pairs.

3.4. Polaron Formation. In our experiments, no distinct formation of polarons was observed for RRa-P3HT films although polaron pairs were observed. The lack of observation of long-lived polarons is consistent with a previous report that the charge formation yield is less than 1%.[17] In contrast to RRa-P3HT, substantial formation of polarons was observed for RR-P3HT films. For the 400 nm excitation, as shown in Figure 9a, the transient signal ascribable to polarons was observed even at 0 ps over the wide excitation intensity range. As is the case in the polaron pair formation, we conclude that polarons are also promptly generated in competition with the vibrational relaxation, from a higher vibrational state in the lowest singlet exciton state under lower photon densities ($<3 \times 10^{18}$ cm^{-3}), and additionally from higher singlet exciton states produced by the singlet exciton−exciton annihilation under higher photon densities ($>3 \times 10^{18}$ cm^{-3}). On the other hand, as shown in Figure 9b, no polarons were observed at 0 ps upon the excitation at 620 nm close to the band edge of the absorption under lower photon densities ($<8 \times 10^{17}$ cm^{-3}) while the yield of polarons increased under higher photon densities ($>8 \times 10^{17}$ cm^{-3}) because of the singlet exciton−exciton annihilation. This finding suggests that polarons are generated from a hot exciton with excess energy. Therefore, such a rapid polaron formation can be basically explained again in terms of the hot-exciton dissociation model as with the polaron pair formation. As shown in Scheme 1, the polaron formation should be in competition with not only the vibrational relaxation of singlet exciton states but also the formation of polaron pairs. To explain the difference in the polaron formation between RRa-P3HT and RR-P3HT in that the formation of polaron pairs is dominant in RRa-P3HT while the formation of polarons is effectively competitive with that of polaron pairs in RR-P3HT, we should consider the different film morphologies between RRa-P3HT and RR-P3HT[7,8] in analogy with the discussion on the formation mechanism for polaron pairs described before. In crystalline RR-P3HT films,

(43) Arkhipov, V. I.; Bässler, H. *Phys. Status Solidi A* **2004**, *201*, 1152–1187.
(44) Scholes, G. D. *ACS Nano* **2008**, *2*, 523–537.

singlet exciton states generated immediately after the laser excitation are considered to be CT excitons containing significant weights of interchain CT configurations because of the larger interchain interaction due to dense π stacking in crystalline domains compared with that in amorphous RRa-P3HT films. The larger interchain interaction strongly mixes quasi-degenerate configurations to form a denser and wider band of CT exciton states, which may form a quasi-continuous band, leading to autoionization from higher singlet exciton states generated by the singlet exciton−exciton annihilation.[44−46] Furthermore, such CT excitons in crystalline domains are likely to be more delocalized than those in amorphous domains and therefore can be dissociated more easily into polarons rather than form tightly bound polaron pairs. Another possible pathway for the polaron formation is dissociation from polaron pairs. As described before, no polaron pairs in RR-P3HT return to the ground state on the picosecond time scale, because the rapid decay of polaron pairs observed (~0.8 ps) was not consistent with the recovery time of the ground-state photobleaching. Thus, the rapid decay of polaron pairs could be ascribed to the dissociation into polarons or to the recombination to the singlet exciton. The recombination to the triplet exciton is ruled out, because polaron pairs should remain singlet in character on such a short time scale and it is too fast for the spin conversion. If most of the polarons were generated not from CT excitons but from polaron pairs, the transient signal at 0 ps would be negligible, and instead a substantial rise would be observed on the same time scale as the decay of polaron pairs (~0.8 ps). However, this is not the case. The transient signal of polarons was observed even at 0 ps and remained constant up to the nanosecond time domain under lower excitation intensities. Therefore, we conclude that polaron pairs cannot be efficiently dissociated into polarons without an applied electric field because of the strong Coulomb attraction but rather recombine to the singlet exciton and that polarons are mainly generated from nonrelaxed CT excitons in competition with the vibrational relaxation and the formation of polaron pairs.

We also consider the formation yield of polarons in RR-P3HT pristine films immediately after the laser excitation. Assuming that the molar absorption coefficient of the polaron band is comparable to that of the singlet exciton band,[17] as shown on the right axis of Figure 9, the polaron yield at 0 ps was roughly estimated under the 400 nm and 620 nm excitation conditions. This assumption is highly probable on the basis of the comparison of each band with the ground-state photobleaching (see the Supporting Information). However, the estimation is the upper limit because the formation of polaron pairs should be taken into account. Under lower excitation intensities, the polaron yields estimated are negligible for the 620 nm excitation and ~6% for the 400 nm excitation. This estimation is consistent with a previous study reporting that the initial photoionization yield is constant at 1.7% within the excitation range of 1.9−3.0 eV and increases to 7% above 3.0 eV.[46] Under higher excitation intensities, the polaron yields increased with increasing excitation intensity and exceeded more than 30% at an excitation density of 2×10^{19} cm^{-3}. As mentioned before, this is because the polaron formation is more efficient from higher exciton states such as CT excitons produced by the singlet exciton−exciton annihilation.

3.5. Triplet Exciton Formation. In RRa-P3HT films, the triplet rise (~4 ps) was in agreement with the singlet decay (~4 ps), suggesting that triplet excitons are rapidly interconverted from singlet excitons. However, this interconversion time, ~4 ps, cannot be explained in terms of ISC from the lowest singlet exciton state to the triplet exciton state, because the ISC rate has been reported to be ~1 ns^{-1} for poly(3-octylthiophene) in a xylene solution.[22] The short lifetime of singlet excitons is due to the singlet exciton−exciton annihilation. Consequently, the rise time of triplet excitons should also be shortened apparently. If the singlet exciton−exciton annihilation deactivates merely singlet excitons and is not related to the formation of triplet excitons, the formation yield of triplet excitons should be reduced significantly. However, we observed a high yield of triplet excitons in RRa-P3HT films even though singlet excitons were quenched by the singlet exciton−exciton annihilation. We estimate the formation yield of triplet excitons to be ~25% at 10 ps from the transient absorption decay (Figure 6a, solid line), assuming that the molar absorption coefficient of the triplet exciton is the same as that of the singlet exciton.[22] On the other hand, if triplet excitons were formed only from singlet excitons via ISC, the triplet yield at 10 ps would be estimated to be as small as ~1% because of the slow ISC rate. We therefore conclude that the rapid triplet formation results from the singlet exciton−exciton annihilation in the picosecond time domain. As shown in Scheme 2, the singlet exciton−exciton annihilation produces a higher singlet exciton state. The triplet formation from a higher exciton state should be completed before the relaxation to the lowest singlet exciton state, because the interconversion in the relaxed exciton states is limited by the slow ISC rate. We therefore conclude that the rapid triplet formation is in competition with the vibrational relaxation to the lowest exciton and polaron pair states, which is as fast as <100 fs. Such a rapid triplet formation is indicative of efficient spin-mixing between singlet and triplet excitons. However, the hyperfine interaction energy, which would play an important role in the interconversion mechanism in organic radicals, is typically on the order of ~5 mT. This corresponds to an interconversion time of several nanoseconds.[47,48] Thus, other mechanisms are needed to explain the ultrafast spin conversion on a short time scale of picoseconds. More probably, the ultrafast triplet formation seems to be the spin-allowed conversion as is discussed below.

Fission of singlet excitons into two triplet exciton pairs is spin-conserving and thus spin-allowed, because six of the nine possible intermediate pair states have singlet character.[45] Triplet formation through the fission of singlet excitons has been reported for molecular crystals,[49−54] and also for conjugated polymer films.[55−57] The energy requirement for the singlet fission has been found to be given by a threshold energy being

(45) Pope, M.; Swenberg, C. E. *Electronic Processes in Organic Crystals and Polymers*; Oxford University Press: Oxford, U.K., 1999.
(46) Dicker, G.; de Haas, M. P.; Siebbeles, L. D. A.; Warman, J. M. *Phys. Rev. B* **2004**, *70*, 045203.
(47) Sheng, Y.; Nguyen, T. D.; Veeraraghavan, G.; Mermer, Ö.; Wohlgenannt, M.; Qiu, S.; Scherf, U. *Phys. Rev. B* **2006**, *74*, 045213.
(48) Verhoeven, J. W. *J. Photochem. Photobiol., C* **2006**, *7*, 40–60.
(49) Singh, S.; Jones, W. J.; Siebrand, W.; Stoicheff, B. P.; Schneider, W. G. *J. Chem. Phys.* **1965**, *42*, 330–342.
(50) Katoh, R.; Kotani, M. *Chem. Phys. Lett.* **1992**, *196*, 108–112.
(51) Merrifield, R. E.; Avakian, P.; Groff, R. P. *Chem. Phys. Lett.* **1969**, *3*, 386–388.
(52) Albrecht, W. G.; Michel-Beyerle, M. E.; Yakhot, V. *Chem. Phys.* **1978**, *35*, 193–200.
(53) Zenz, C.; Cerullo, G.; Lanzani, G.; Graupner, W.; Meghdadi, F.; Leising, G.; Silvestri, S. D. *Phys. Rev. B* **1999**, *59*, 14336–14341.
(54) Katoh, R.; Kotani, M.; Hirata, Y.; Okada, T. *Chem. Phys. Lett.* **1997**, *264*, 631–635.
(55) Österbacka, R.; Wohlgenannt, M.; Shkunov, M.; Chinn, D.; Vardeny, Z. V. *J. Chem. Phys.* **2003**, *118*, 8905–8916.

equivalent to two thermalized triplet excitons ($2E_{T1}$).[52] The energy level of the lowest triplet exciton state (E_{T1}) is roughly estimated to be 1.6 eV for RRa-P3HT amorphous films and 1.55 eV for RR-P3HT crystalline films from that of the lowest singlet exciton state (E_{S1}) and the energy gap between E_{S1} and E_{T1} (ΔE_{ST}). The energy level of the lowest singlet exciton state was evaluated from the absorption and emission spectra of the two films: $E_{S1} = 2.3$ eV for RRa-P3HT and $E_{S1} = 2.0$ eV for RR-P3HT. The singlet−triplet splitting energy ΔE_{ST} has been reported to be 0.7 eV for various amorphous conjugated polymers[58,59] and 0.45 eV for highly ordered poly(3-octylthiophene) films.[60] Assuming that ΔE_{ST} is 0.7 eV for RRa-P3HT and 0.45 eV for RR-P3HT, therefore, a threshold energy for the singlet fission is estimated to be 3.2 eV for RRa-P3HT and 3.1 eV for RR-P3HT. Both energy levels are comparable to or slightly higher than the excitation energy (3.1 eV). Therefore, the singlet fission by one photon excitation at 400 nm is thermodynamically unfavorable for both polymers, which is consistent with our transient results that neither RRa-P3HT nor RR-P3HT exhibited distinct triplet signals immediately after the laser excitation under lower excitation intensities. On the other hand, the singlet fission is thermodynamically possible for both polymers from a higher singlet exciton state generated by the singlet exciton−exciton annihilation (singlet fusion). If triplet excitons are generated through the singlet fission, the back-recombination of triplet exciton pairs to the singlet exciton state is also spin-allowed and therefore expected to be much faster than the normal spin-forbidden transition from triplet excitons to the ground state. As shown in Figure 6, the lifetime of triplet signals observed for RRa-P3HT was as short as 300 ps, which is much faster than that of isolated triplet excitons (>μs). This rapid decay is ascribed to the recombination of triplet exciton pairs to the singlet exciton state. Therefore, as shown in Scheme 2, we conclude that triplet excitons observed for RRa-P3HT films are mainly generated through the singlet fission from a higher singlet exciton state produced by the singlet exciton−exciton annihilation (singlet fusion followed by singlet fission into triplet exciton pairs).

In contrast to RRa-P3HT, no triplet formation was observed for RR-P3HT. This is probably because the formation of polarons or polaron pairs is more efficient than that of the singlet fission because of the larger interchain interaction in highly ordered crystalline RR-P3HT films, as shown in Scheme 1, which may form a quasi-continuous band, leading to autoionization from higher singlet exciton states generated by the singlet exciton−exciton annihilation. For perylene crystals, the fission threshold energy has been reported to be dependent upon the crystalline morphology.[52] The excimer-forming α-crystal has a larger fission threshold energy than the monomeric β-crystal. The larger threshold energy is attributed to faster excimer formation competing with the singlet fission in the α-crystal. This is analogous to our conclusion that the polaron formation is more efficient than the singlet fission in highly ordered RR-P3HT films where the π conjugation plane of the main chain is stacked like the molecular alignment in the α-perylene crystal, while the singlet fission is dominant in RRa-P3HT films where the π conjugation plane of the main chain is not ordered, which is rather similar to the molecular alignment in the β-perylene crystal. Therefore, we conclude that the competition of the singlet fission with the polaron formation in conjugated polymers is highly dependent upon the film morphology.

3.6. Relevance to Polymer Solar Cells. Finally, we mention the relevance of the photophysics discussed above to polymer solar cells. First, we should note that polarons can be generated from a hot exciton in pristine RR-P3HT bulk films even in the absence of electric fields. In general, excitons generated in polymer solar cells are considered to be dissociated into free carriers only at the heterojunction.[5] Recently, however, several groups have reported that polarons may be generated not only at the heterojunction but also in the P3HT bulk films.[17−20] Our findings support these previous reports and furthermore demonstrate that hot excitons play an important role in the formation mechanism of polarons. Most recently a power conversion efficiency of ∼2% has been reported for a bilayer device of RR-P3HT and PCBM.[61] Interestingly, the bilayer device exhibits the best device performance when the RR-P3HT layer is as thick as 65 nm. Considering the exciton diffusion length of singlet excitons as short as ∼8 nm as reported previously,[62] this result suggests that excitons can be dissociated into free polarons in the RR-P3HT bulk layer. Although from our transient study the formation yield of polarons from a hot exciton is estimated to be as small as a few percent in RR-P3HT pristine films, it could be enhanced under applied electric fields such as a short-circuit condition. We separately estimate the dissociation yield of hot excitons under different electric fields on the basis of the Onsager−Braun model.[63−65] The estimation suggests that the polaron yield could be enhanced from a few percent in the absence of the electric field to several tens of percent under the short-circuit condition where the internal electric field is $\sim 10^7$ V m^{-1} (see the Supporting Information). This is a preliminary calculation, and therefore, further experiments are needed to prove the electric-field dependence of the polaron yield. Nevertheless, this estimation is indicative of potential relevance to polaron generation from hot excitons in the polymer bulk. Further experiments to examine the electric-field dependence are currently in progress.

Next, we should note the relevance of the singlet fission into two triplets to polymer solar cells. As mentioned before, the singlet exciton fission produces two triplet excitons from a higher singlet exciton. This phenomenon is similar to multiple exciton generation in semiconductor quantum dots,[66] which has attracted much attention because more than one exciton could be generated upon the absorption of one photon. Recently, the possibility of the singlet fission of organic dyes to improve the efficiency of dye-sensitized solar cells has been theoretically introduced.[67] In RRa-P3HT films, the singlet exciton fission is not directly linked with the polaron formation. This is partly because the triplet exciton state is located lower in energy than

(56) Wohlgenannt, M.; Graupner, W.; Leising, G.; Vardeny, Z. V. *Phys. Rev. Lett.* **1999**, *82*, 3344–3347.
(57) Kraabel, B.; Hulin, D.; Aslangul, C.; Lapersonne-Meyer, C.; Schott, M. *Chem. Phys.* **1998**, *227*, 83–98.
(58) Köhler, A.; Wilson, J. S.; Friend, R. H.; Al-Suti, M. K.; Khan, M. S.; Gerhard, A.; Bässler, H. *J. Chem. Phys.* **2002**, *116*, 9457–9463.
(59) Köhler, A.; Beljonne, D. *Adv. Funct. Mater.* **2004**, *14*, 11–18.
(60) Sakurai, K.; Tachibana, H.; Shiga, N.; Terakura, C.; Matsumato, M.; Tokura, Y. *Phys. Rev. B* **1997**, *56*, 9552–9556.
(61) Kim, B. J.; Miyamoto, Y.; Ma, B.; Fréchet, J. M. J. *Adv. Funct. Mater.* **2009**, *19*, 2273–2281.
(62) Shaw, P. E.; Ruseckas, A.; Samuel, I. D. W. *Adv. Mater.* **2008**, *20*, 3516–3520.
(63) Onsager, L. *Phys. Rev.* **1938**, *54*, 554–557.
(64) Braun, C. L. *J. Chem. Phys.* **1984**, *80*, 4157–4161.
(65) Marsh, R. A.; McNeill, C. R.; Abrusci, A.; Campbell, A. R.; Friend, R. H. *Nano Lett.* **2008**, *8*, 1393–1398.
(66) Nozik, A. J. *Chem. Phys. Lett.* **2008**, *475*, 3–11.
(67) Paci, I.; Johnson, J. C.; Chen, X.; Rana, G.; Popovic, D.; David, D. E.; Nozik, A. J.; Ratner, M. A.; Michl, J. *J. Am. Chem. Soc.* **2006**, *128*, 16546–16553.

the polaron state. In other words, we should consider other factors such as the energy level alignment to realize the effective contribution of the singlet exciton fission to the photocurrent generation. Nonetheless, we emphasize that the internal quantum efficiency might have a chance to exceed unity if triplet excitons generated through the singlet fission can be efficiently dissociated into free polarons. Our finding suggests that the singlet exciton fission would occur more efficiently in amorphous polymer films such as RRa-P3HT rather than in crystalline polymer films such as RR-P3HT. This would be a guideline to design new polymers in which the singlet exciton fission occurs more efficiently.

4. Conclusions

We have comprehensively studied a series of fundamental photophysical processes from exciton delocalization to ultrafast formation of polaron pairs, polarons, and triplet excitons in RRa-P3HT and RR-P3HT pristine films by transient absorption spectroscopy over the wide wavelength region from 500 to 1650 nm under various excitation intensities. On the basis of these detailed analyses, we obtained several important findings: the correct assignments of transient spectra, the estimation of exciton delocalization radii, and the formation dynamics of polaron pairs, polarons, and triplet excitons in P3HT films as follows. For RRa-P3HT films, we observed three characteristic absorption bands: singlet excitons (~1000 nm), polaron pairs (~700 nm), and triplet excitons (~800 nm). Immediately after the laser excitation singlet excitons and polaron pairs were generated promptly, and subsequently triplet excitons were rapidly generated in a few picoseconds. The triplet rise was the same as the singlet exciton decay but much faster than the normal intersystem crossing. The delocalization radius of singlet excitons is estimated to be ~3.2 nm immediately after the laser excitation at 400 nm and increased with time. No polaron pairs were observed upon the excitation at 500 nm close to the band gap of RRa-P3HT. Therefore, we conclude that polaron pairs are generated from hot excitons in competition with rapid vibrational relaxation such as the dynamic localization of the singlet exciton and more efficiently from higher hot excitons produced by the singlet exciton−exciton annihilation under higher excitation conditions. The relatively high anisotropy of the polaron pair band up to the nanosecond time domain indicates that polaron pairs are so tightly bound that they cannot migrate freely but are rather likely to decay by geminate recombination. For RR-P3HT films, we observed three characteristic absorption bands: singlet excitons (~1200 nm), polaron pairs (~650 nm), and polarons (~1000 nm). All these transient species were generated immediately after the laser excitation. The delocalization radius of singlet excitons at 0 ps is estimated to be ~4.3 nm for the 400 nm excitation and ~6.7 nm for the 620 nm excitation, indicating that more delocalized singlet excitons are formed in the RR-P3HT film compared with the RRa-P3HT film because of the strong interchain interaction. Neither polaron pairs nor polarons were observed immediately after the laser excitation upon the excitation at 620 nm close to the band gap of RR-P3HT. We therefore conclude that polaron pairs and polarons are generated from hot excitons in competition with the rapid vibrational relaxation of the singlet exciton and more efficiently from higher hot excitons produced by the singlet exciton−exciton annihilation under higher excitation conditions. The polaron pairs decayed monomolecularly, indicating that polaron pairs are tightly bound and therefore decay to the singlet exciton by geminate recombination. In contrast, the polarons decayed bimolecularly, indicating that polarons can migrate freely and recombine with other polarons. These observations suggest that hot excitons play a crucial role in the effective formation of polaron pairs and polarons in P3HT bulk films, which could be enhanced under the short-circuit condition and therefore would have potential relevance to charge generation in polymer solar cells. On the other hand, we should note that triplet excitons are efficiently generated on a picosecond time scale in RRa-P3HT films while polarons are generated in RR-P3HT films instead of triplet excitons. The rapid triplet formation can be explained by the singlet exciton−exciton annihilation (singlet fusion) followed by the singlet fission into triplet exciton pairs. This is a spin-allowed process and is thermodynamically favorable under the condition that singlet exciton states produced by the singlet fusion are enough higher in energy to provide two triplet excitons. Although this thermodynamic condition is true for RR-P3HT, no triplet formation was found, and instead efficient polaron formation was observed. The remarkably different formation dynamics in two polythiophene films with different regioregularities is probably due to the different singlet excitons generated upon the photoexcitation resulting from the different film morphology of the polymers. In amorphous films of RRa-P3HT, singlet excitons are likely to be localized on intrachains and hence lead to the triplet exciton formation. In highly ordered crystalline films of RR-P3HT, singlet excitons are likely to be delocalized, more mixed with interchain CT states, and therefore dissociated into polarons efficiently. This finding suggests that the singlet exciton fission would occur more efficiently in amorphous polymer films such as RRa-P3HT rather than in crystalline polymer films such as RR-P3HT. This would be contributory to designing new polymers in which the singlet exciton fission occurs more efficiently.

Acknowledgment. This work was partly supported by the Kansai Research Foundation for Technology Promotion, a Grant-in-Aid for Young Scientists (B) (No. 18750100), and the Global COE Program (International Center for Integrated Research and Advanced Education in Materials Science) from the Ministry of Education, Culture, Sports, Science, and Technology of Japan.

Supporting Information Available: Details about the sample preparation, measurements, crystallinity of P3HT films, spectral analysis of transient absorption, estimation of the molar absorption coefficient of singlet excitons and polarons, and estimation of the electric-field dependence of the hot-exciton dissociation yield. This material is available free of charge via the Internet at http://pubs.acs.org.

JA906621A